Design of a varactor-tunable metamaterial absorber*

Lin Bao-Qin(林宝勤)†, Da Xin-Yu(达新宇), Zhao Shang-Hong(赵尚弘), Meng Wen(蒙 文), Li Fan(李 凡), Fang Ying-Wu(方英武), and Wang Jia-Fu(王甲富)

Institute of Information and Navigation, Air Force Engineering University, Xi'an 710077, *China*

(Received 6 October 2013; revised manuscript received 21 December 2013; published online 10 April 2014)

In this paper, we design a varactor-tunable metamaterial absorber (MA). The tunable MA is based on a mushroom-type high impedance surface (HIS), in which varactors are loaded between adjacent metal patches to adjust the capacitance and tune the resonance frequency, the primary ground plane is etched as the bias network to bias all of the varactors in parallel, and another ultra-thin grounded film is attached to the bottom. Its absorption characteristics are realized for electrically dielectric loss. The simulated values of a sample indicate that a tunable frequency range from 2.85 GHz to 2.22 GHz is achieved by adjusting the varactor capacitance from 0.1 pF to 2.0 pF, and better than 0.97 absorbance is realized; in addition, the tunable frequency range is expanded from 4.12 GHz to 1.70 GHz after optimization.

Keywords: metamaterial absorber (MA), high impedance surfaces (HISs), varactor

PACS: 78.20.Ci, 42.25.Bs **DOI:** 10.1088/1674-1056/23/6/067801

1. Introduction

Electromagnetic metamaterials[1] are artificially designed media, which exhibit unique electromagnetic properties that are unattainable for natural materials, such as negative permittivities,[2] permeabilities,[3] refractive indices,[4,5] electromagnetic band-gaps,[6,7] high impedance properties,[8] and invisibilities.[9] Due to the peculiar electromagnetic properties, the designs and applications of metamaterials have attracted much attention. In recent years, novel designs of resonant metamaterial absorbers (MAs) have been proposed.[10–18]

The perfect absorption of an MA is mainly due to the local electromagnetic resonance mechanism. By adjusting the design value of the unit cell, its electromagnetic response can be tuned independently, and the impedance of the structure can be matched to that of free space at the resonance frequency. Thus, a "perfect" absorber with near-unity absorbance can be realized.

Most up-to-date MAs are composed of metallic electric resonators and cut wires or metallic ground plates. These ultra-thin MAs comprising metallic ground plates have in-phase reflection characteristics for incident plane waves, which are just based on the metamaterial's high impedance property. These metamaterials with high impedance property are usually realized by placing periodic metallic arrays in front of ultrathin grounded substrates, which are often referred to as high impedance surfaces (HISs).

MAs are strongly dependent on electromagnetic resonances, and their bandwidths are often narrow, typically no more than 10% with respect to the central frequency. The narrow bandwidth features of resonant absorption restrict the practical applications of these MAs. To improve the performances of the MAs in practical application, recently studies of active MAs have been conducted. A well-established method for tuning an MA is to incorporate electronically tunable components into its unit cells. A limited number of electronically tunable MAs have been designed using solid-state varactor diodes.[19–24] For biasing the varactor diodes, the tunable MA requires separate circuitry as bias network. Because of the effect of the bias network on the MA frequency response, biasing the varactor diodes properly is a major difficulty in designing a tunable MA.

In this paper, one varactor-tunable MA is designed. It is based on a mushroom-type HIS with electrically dielectric loss, in which the tunability is achieved by connecting adjacent patches with varactors, and the proper bias network is designed on the primary ground plane. The absorption property of the tunable absorber is demonstrated through numerical simulations.

2. Design and optimization

A conventional mushroom-type HIS consists of a doubly periodic array of metal patches with grounding vias shown in Fig. 1. This metasurface can be modeled as a parallel LC resonant circuit as shown in Fig. 1(b), where the effective inductance L results from the magnetic field above the ground surface, and the effective capacitance C comes from the electric field between adjacent metal patches. At the resonance frequency, the surface impedance of this metasurface is infinity, it just behaves as an artificial magnetic conductor (AMC), and strong electric fields are brought about in the surface for the in-phase reflection, so this metasurface can realize an effective electromagnetic absorption and be used as an MA when

*Project supported by the National Natural Science Foundations of China (Grant Nos. 61271250 and 11204378).

†Corresponding author. E-mail: aflbq@sina.com

© 2014 Chinese Physical Society and IOP Publishing Ltd

electrically lossy dielectric or resistance is introduced.

The resonance frequency of an HIS can be tuned by adjusting the values of its effective circuit parameters. A limited number of varactor-tunable mushroom-type HISs are presented in Refs. [25]–[27]. In this work, to construct a novel tunable MA using HIS, we start with designing a varactor-tunable HIS.

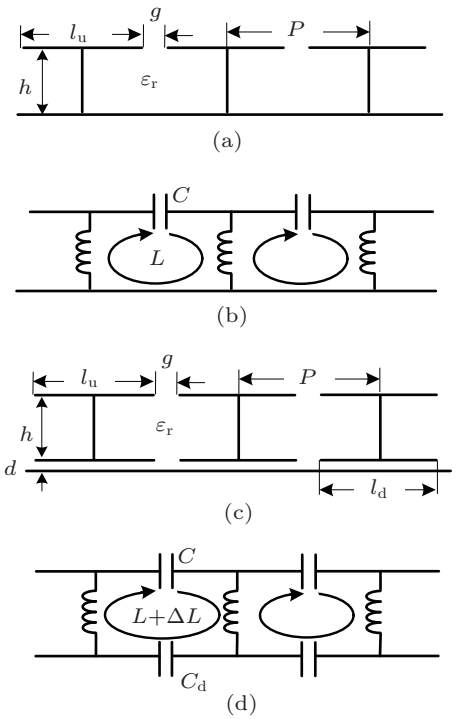


Fig. 1. Sievenpiper mushroom-type HIS structure (a) and its equivalent circuit (b); the proposed transformative HIS structure (c) and its equivalent circuit (d).

2.1. Varactor-tunable HIS

When varactors are loaded between the adjacent patches in the periodic surface texture of a mushroom-type HIS, the varactor capacitance C_{Var} is just merged with the distributed capacitance C between the adjacent patches, such that the resonance frequency of the local electromagnetic resonance can be tuned effectively if the loaded varactors were reversely biased. The varactor-tunable HISs in Refs. [25] and [26] are realized in different biased manners. We design a varactor-tunable HIS in a simple and effective biased manner, and the design process is described in detail as follows.

First, we suppose that a kind of varactor is loaded between the adjacent patches in a mushroom-type HIS as shown in Ref. [26]. To construct a proper bias network for the varactors, we design a transformative HIS structure. In the conventional HIS, all of the metal patches with grounding vias are electrically connected, while the adjacent patches will be electrically separated to introduce DC bias voltages. Now we etch the ground plane into a square patch array, which is just similar to the one on the upper surface texture, and then attach another ultra-thin grounded film to the bottom as shown in Fig. 1(c). In this way, each cell in the transformative HIS is electrically independent, and another distributed capacitance C_{d} between the adjacent patches on the nether surface is strung into the equivalent resonant circuit as shown in Fig. 1(d), in addition, the effective inductance L has a little increment ΔL because of the incrassation of the HIS structure. The nether-distributed capacitance C_{d} is much larger than the upper one C for the ultra-thin grounded film, which mostly comes from two series-wound parallel plate capacitors which comprise a parallel square patch and the ground plane, while the increment ΔL of effective inductance L is very small for the attached grounded film is ultra-thin. So the resonance frequency of the transformative HIS can be expressed as:

$$\omega = \sqrt{\frac{1+C/C_{\mathrm{d}}}{(L+\Delta L)C}} \approx \sqrt{\frac{1}{LC}}. \tag{1}$$

It is indicated that the structural transformation in the transformative HIS has little effect on the local electromagnetic resonance, and the resonance frequency almost keeps the same as that of the primary mushroom-type HIS.

To demonstrate the properties of the transformative HIS, we construct a sample based on a primary mushroom-type HIS. The structural parameters of the primary HIS are as follows: $P = 25.0$ mm, $l_{\mathrm{u}} = 23.8$ mm, $g = 1.2$ mm, $h = 0.5$ mm, and $\varepsilon_{\mathrm{r}} = 4.4$. In the transformative one, the primary ground plane is etched into a square array of metal patch with a width $l_{\mathrm{d}} = 23.8$ mm, and the attached ultra-thin grounded film has thickness $d = 0.1$ mm and relative permittivity $\varepsilon_{\mathrm{r}} = 1.8$. Now we suppose that they are both loaded with a kind of tunable capacitor with capacitance C_{Tu} as shown in Ref. [26]. When C_{Tu} is assumed to be different values, by using Ansoft HFSS software, the simulated reflection phases in the case of normal incidence are shown in Fig. 2.

The phase diagram in Fig. 2 shows that in-phase reflections occur in both HISs. When C_{Tu} is assumed to be 0.0 pF, their reflection phases are almost the same. With capacitance C_{Tu} increasing from 0.0 pF to 2.0 pF, the resonance frequency of the primary mushroom-type HIS, where the reflection phase is just equal to zero, decreases from 2.88 GHz to 2.27 GHz, while that of the transformative HIS is tuned at a faster rate, and it decreases to 2.21 GHz when $C_{\mathrm{Tu}} = 2.0$ pF. To explain this cause, now we express the resonance frequency ω_{t} of the transformative HIS after the tunable capacitors have been loaded as follows:

$$\begin{aligned}\omega_{\mathrm{t}} &= \sqrt{\frac{1+(C+C_{\mathrm{Tu}})/C_{\mathrm{d}}}{(L+\Delta L)(C+C_{\mathrm{Tu}})}} \\ &= \sqrt{\frac{1}{(L+\Delta L)(C+C_{\mathrm{Tu}})}+\frac{1}{(L+\Delta L)C_{\mathrm{d}}}},\end{aligned} \tag{2}$$

while that of the primary mushroom-type one, ω_m, is

$$\omega_m = \sqrt{\frac{1}{L(C+C_{Tu})}}. \quad (3)$$

When C_{Tu} is assumed to be zero, $\omega_t \approx \omega_m$ for the larger C_d and the smaller ΔL. With the increase of C_{Tu}, for the primary HIS, the denominator of ω_m^2 increases with C_{Tu} multiplied by a coefficient L; while for the transformative HIS, ω_t^2 is the sum of two parts as formula (2), the second part is smaller and invariable, and the denominator of the first part of formula (2) increases with C_{Tu} multiplied by a bigger coefficient $(L+\Delta L)$, and now it is clear why ω_t decreased at a faster rate.

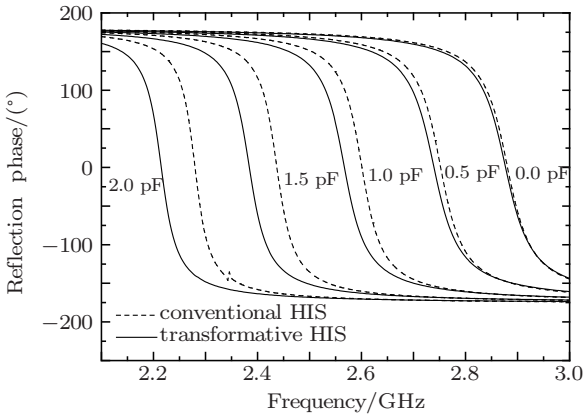


Fig. 2. Reflection phase of the transformative HIS, together with those of the primary mushroom-type one.

In succession, a varactor-tunable HIS is constructed expediently based on the proposed transformative one. We load a kind of varactor in the transformative HIS as shown in Fig. 3(a). To apply a DC bias voltage to each varactor, we introduce one vertical metallic strip with width $w = 0.4$ mm between each pair of adjacent rows in the nether patch array, the metallic strip is connected to the adjacent patches alternately from side to side as shown in Fig. 3(b). Now all of the varactors are reversely biased in parallel when DC voltage is applied between the adjacent metallic strips. In addition, these connections increase a small amount of the distributed capacitance C_d between the adjacent patches, and slightly reduce the inductance increment ΔL for the effect of short circuit between the far-between patches. So, on the right-hand side of formula (2), the first part of ω_t^2 will increase, while the second one will decrease: both change very little, indicating that the resonance frequency will nearly keep the same as that of the transformative HIS. In this way, a novel varactor-tunable HIS is obtained, its lengthwise cross section is shown in Fig. 3(c). As the simulated results, its reflection phases and those of the above transformative HIS are shown in Fig. 4.

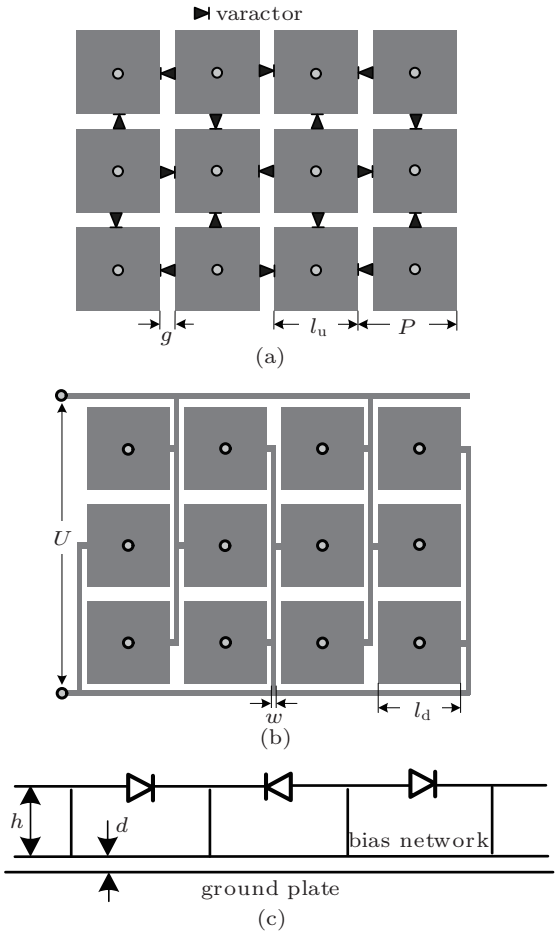


Fig. 3. Designed varactor-tunable HIS: (a) top view, (b) bias network, and (c) lengthwise cross section.

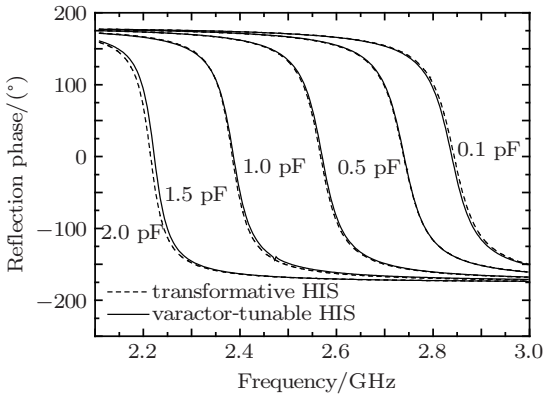


Fig. 4. Simulated results of reflection phase in cases of different values of varactor capacitance for the varactor-tunable HIS.

In Fig. 4, it is shown that the resonant frequency of the tunable HIS is dominated by the varactor capacitance C_{Var}, it is tuned in a frequency range from 2.85 GHz to 2.22 GHz when C_{Var} changes from 0.1 pF to 2.0 pF, and the reflection phase is almost the same as that of the transformative HIS loaded with the same capacitance. Under careful inspection it is found that the resonant frequency is slightly reduced when $C_{Var} = 0.1$ pF due to the augment of the capacitance C_d, and the control rate is also slightly reduced because of the reduction of the inductance increment ΔL.

2.2. Varactor-tunable MA

The proposed varactor-tunable HIS can realize in-phase reflection at different resonance frequencies with the variation of the varactor capacitance $C_{\rm Var}$. At the resonance frequency, the HIS behaves as an AMC, and strong electric fields are brought in the ultra-thin structure. It is indicated that the electromagnetic energy will be dissipated if electrically lossy dielectric or resistance is introduced. So we construct a tunable MA expediently based on the proposed varactor-tunable HIS. Now we replace the upper dielectric layer in the above varactor-tunable HIS by a lossy FR4 dielectric layer, whose relative permittivity is kept to be $\varepsilon_{\rm r} = 4.4$, while the loss tangent is changed into $\tan\delta = 0.025$. When $C_{\rm Var}$ is assumed to be different values, the absorbance of the varactor-tunable HIS is shown in Fig. 5.

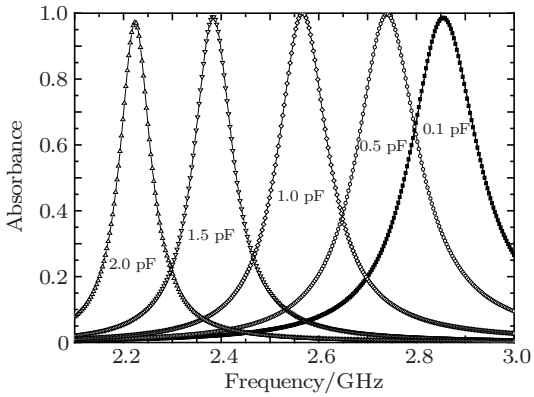


Fig. 5. Variations of absorbance with frequency of the varactor-tunable MA at several different values of $C_{\rm Var}$.

Figure 5 shows that better than 0.97 absorbance is realized in each case; in addition, the resonant frequency, where the best absorbance is realized, remains the same as that of the varactor-tunable HIS. It is reduced from 2.85 GHz to 2.22 GHz with capacitance $C_{\rm Var}$ increasing from 0.1 pF to 2.0 pF. It is indicated that a varactor-tunable MA is designed successfully.

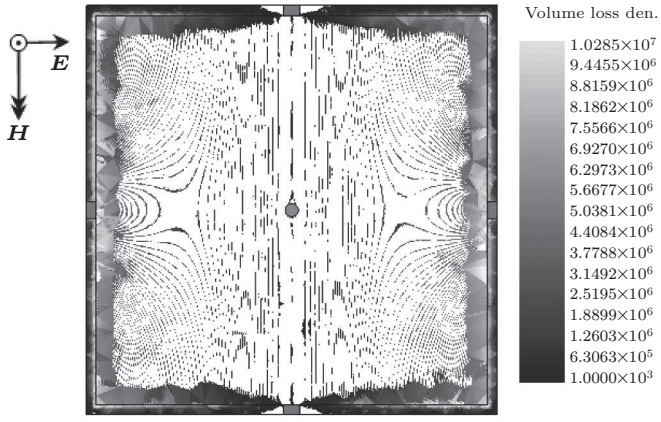


Fig. 6. (color online) Power loss density (den.) distribution in a unit cell of the varactor-tunable MA ($C_{\rm Var} = 1.0$ pF).

To gain a better physical insight into the absorption properties of the varactor-tunable MA, when the varactor capacitance $C_{\rm Var}$ is assumed to be 1.0 pF, the power loss density distribution in one unit cell is shown in Fig. 6. It is clear that the power loss mainly concentrates in the area near the gap between two metallic patches in adjacent cells, indicating that there are strong electric fields in these areas. That is just because the gap, acting as a capacitor in a resonant circuit, has cut off the resonant electric current, which leads to the electric charge accumulation at the edges of these patches.

2.3. Optimization of varactor-tunable MA

Finally, to increase the tunable frequency range of the varactor-tunable MA, we realize an effective optimization for it. According to formula (2), when we ignore the little effect of capacitance $C_{\rm d}$, the cover coefficient of frequency changing with $C_{\rm Var}$ can be expressed as

$$I = \frac{\omega_{\max}}{\omega_{\min}} = \sqrt{\frac{C + C_{\rm Varmin} + \Delta C_{\rm Var}}{C + C_{\rm Varmin}}} = \sqrt{1 + \frac{\Delta C_{\rm Var}}{C + C_{\rm Varmin}}}. \quad (4)$$

It is indicated that reduction of the distributed capacitance C can augment the cover coefficient effectively.

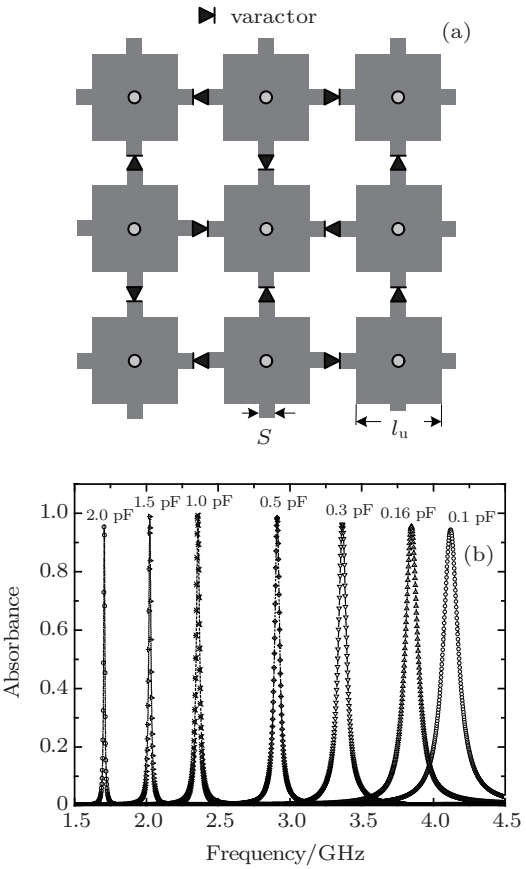


Fig. 7. Optimized tunable MA: (a) top view and (b) the absorbance versus frequency.

The distributed capacitance C is just between the adjacent patches on the upper surface texture. Now the upper patch array in the optimized tunable MA is changed as shown in Fig. 7(a), where the width S of the strips connected with the varactor is kept to be $S = 1.0$ mm. Such a reduction in width $l_{\rm u}$

of each patch will reduce the distributed capacitance C, and the tunable frequency range can be expanded effectively. When the width is reduced into $l_u = 13.0$ mm, the simulated results are shown in Fig. 7(b).

Figure 7(b) shows that the resonant frequency is reduced from 4.12 GHz to 1.70 GHz as capacitance C_{Var} increases from 0.1 pF to 2.0 pF, and the cover coefficient of frequency change is augmented up to 2.42. In addition, better than 0.94 absorbance has been realized in each case.

3. Conclusion

In this work, an effective approach to the design of a varactor-tunable MA is presented. The tunable MA is based on a mushroom-type high impedance surface (HIS), in which varactors are loaded between adjacent metal patches, and the primary ground plane is etched into the bias network. In addition, the proper electrically dielectric loss is introduced to realize the absorption. The frequency tuning capability of the proposed MA is demonstrated through numerical simulations. The resonant frequency is tuned from 2.85 GHz to 2.22 GHz by adjusting the varactor capacitance from 0.1 pF to 2.0 pF, and better than 0.97 absorbance is realized in each case; in addition, the tunable frequency range is expanded from 4.12 GHz to 1.70 GHz after optimization.

References

[1] Caloz C and Itoh T 2006 *Electromagnetic Metamaterials: Transmission Line Theory and Microwave Applications* (New Jersey: John Wiley & Sons, Inc.) p. 2

[2] Pendry J B, Holden A J, Stewart W J and Youngs I 1996 *Phys. Rev. Lett.* **76** 4773

[3] Pendry J B, Holden A J, Robbins D J and Stewart W J 1999 *IEEE Trans. Microwave Theory Technol.* **47** 2075

[4] Veselago V G 1968 *Sov. Phys. Usp.* **10** 509

[5] Shelby R A, Smith D R and Schultz S 2001 *Science* **292** 77

[6] Sievenpiper D, Zhang L, Broas R F J, Alexopoulos N G and Yablonovitch E 1999 *IEEE Trans. Microwave Theory Technol.* **47** 2059

[7] Zhou L and Chan C T 2004 *Appl. Phys. Lett.* **84** 1444

[8] Yang F and Rahmat-Samii Y 2003 *IEEE Trans. Anten. Propag.* **51** 2691

[9] Schurig D, Mock J J, Justice B J, Cummer S A, Pendry J B, Starr A F and Smith D R 2006 *Science* **314** 977

[10] Tao H, Bingham C M, Strikwerda A C, Pilon D and Shrekenhamer D 2008 *Phys. Rev. B* **78** 241103

[11] Avitzour Y, Urzhumov Y A and Shvets G 2009 *Phys. Rev. B* **79** 045131

[12] Landy N I, Bingham C M, Tyler T, Jokerst N, Smith D R and Padilla W J 2009 *Phys. Rev. B* **79** 125104

[13] Gu C, Qu S B, Pei Z B, Zhou H, Xu Z, Bai P, Peng W D and Lin B Q 2010 *Chin. Phys. Lett.* **27** 117802

[14] Gu C, Qu S B, Pei Z and Xu Z 2011 *Chin. Phys. B* **20** 037801

[15] Cheng Y Z, Gong R Z, Nie Y and Wang X 2012 *Chin. Phys. B* **21** 127801

[16] Cheng Y Z, Nie Y, Gong R Z, Zheng D H, Fan Y N, Xiong X and Wang X 2012 *Acta Phys. Sin.* **61** 134101 (in Chinese)

[17] Nie Y, Cheng Y Z and Gong R Z 2013 *Chin. Phys. B* **22** 044102

[18] Lu L, Qu S B, Su X, Shang Y, Zhang J and Bai P 2013 *Acta Phys. Sin.* **62** 208103 (in Chinese)

[19] Mias C 2003 *Electron. Lett.* **39** 1060

[20] Yap J H and Mias C 2005 *IEE Wideband and Multi-band Antennas and Arrays* **7** 171

[21] Satoshi Y, Keigo K, Masayuki N, Yoshiyuki Y and Hirokazu S 2011 *IEICE Trans. Commun.* **94** 2306

[22] Costa F and Vastante G P 2011 *IEEE Antennas and Wireless Propagation Letters* **10** 11

[23] Yang Y J, Huang Y J, Wen G J, Zhong J P and Sun H B 2012 *Chin. Phys. B* **21** 038501

[24] Zhao J, Cheng Q, Chen J, Mei Q Q, Wei X J and Tie J C 2013 *New J. Phys.* **15** 043049

[25] Mias C and Yap J H 2007 *IEEE Trans. Anten. Propag.* **55** 1955

[26] Sievenpiper D F, Schaffner J H, Song H J, Loo R Y and Tangonan G 2003 *IEEE Trans. Anten. Propag.* **51** 2713

[27] Sievenpiper D F and Schaffner J H 2002 *Electron. Lett.* **38** 1237